Journal of Nuclear Materials 466 (2015) 343–350

Contents lists available at ScienceDirect

Journal of Nuclear Materials

journal homepage: www.elsevier.com/locate/jnucmat

Impurity migration and effects on vacancy formation enthalpy in polycrystalline depleted uranium

K.R. Lund [a,*], K.G. Lynn [a], M.H. Weber [a], C. Macchi [b,c], A. Somoza [b,d], A. Juan [c,e], M.A. Okuniewski [f]

[a] Washington State University, Center for Materials Research, Pullman, WA, 99163, USA
[b] Instituto de Física de Materiales Tandil, CIFICEN (CONICET-UNCPBA), Pinto 399, B7000GHG, Tandil, Argentina
[c] Consejo Nacional de Investigaciones Científicas y Técnicas (CONICET), Argentina
[d] Comisión de Investigaciones Científicas de la Provincia de Buenos Aires (CICPBA), Argentina
[e] Instituto de Física del Sur (IFISUR, UNS-CONICET), and Departamento de Física, Universidad Nacional del Sur, Av. Alem 1253, B8000CPB, Bahía Blanca, Argentina
[f] Idaho National Laboratory, Idaho Falls, ID, 83401, USA

ARTICLE INFO

Article history:
Received 13 September 2014
Received in revised form
3 June 2015
Accepted 7 August 2015
Available online 14 August 2015

Keywords:
Positrons
Formation enthalpy
Depleted uranium
Antimatter
Materials properties
Annihilation
Positron annihilation spectroscopy

ABSTRACT

We have used Doppler-broadening of the positron-electron annihilation radiation technique and VASP calculations to verify the previously reported vacancy formation enthalpy H_v^f in polycrystalline depleted uranium. Experimentally we have confirmed a H_v^f of (1.6 ± 0.2) eV. VASP calculations using GGA and LDA approximations gave vacancy formation enthalpies values of 1.98 eV and 2.22 eV respectively. We found residual oxygen in the sample diminished these values by 50% or more. Our new experimental and theoretical data supports the notion that oxygen impurities in the sample are responsible for lower values of vacancy formation enthalpies. Measured and calculated vacancy formation enthalpies, as well as the obtained oxygen migration enthalpy of (0.6 ± 0.1) eV, are compared and discussed with values reported in the literature.

1. Introduction

Metallic uranium and various uranium oxides have been studied with theoretical and experimental techniques to better characterize the elemental properties. Pure uranium has three phases from ambient temperature up to its melting point of 1407 K [1–3] (see Table 1). The γ phase of uranium is stable only at high temperatures and is thermodynamically unstable at low temperatures [4]. When alloyed with Zr or Mo, the bcc γ phase can become stable at lower temperatures. A stable γ phase is desired for reactor engineering and design due to its isotropic swelling behavior [4,5].

Positron annihilation spectroscopy (PAS) techniques have been used to characterize defect properties in uranium. Doppler-Broadening of the Annihilation Radiation (DBAR) enables calculations of vacancy concentration and formation enthalpies [6,7]. Matter et al. [1] and Kögel et al. [2] studied relatively large cylinders (3451 mm^3 for Kögel and 3015 mm^3 for Matter) of polycrystalline uranium samples. After annealing to remove stresses, strains, and impurities, they employed DBAR to extract the vacancy formation enthalpy. Both authors observed discontinuities in their data at phase transition temperatures but with differing values in their measured enthalpies; Matter et al. is 400% larger than that measured by Kögel et al.

As suggested in our previous work [8], it is possible the discrepancies between the two measured vacancy formation enthalpies could be due to the oxygen impurities remaining in their larger samples.

In fact, Matter briefly discussed that the impurities in his sample would generally lead to an enthalpy value smaller than for the pure metallic uranium. With this understanding, he estimated the true value of the formation enthalpy would lie somewhere between 1 and 1.3eV.

* Corresponding author.
E-mail address: kasey.lund@email.wsu.edu (K.R. Lund).

http://dx.doi.org/10.1016/j.jnucmat.2015.08.014
0022-3115/

High-resolution X-ray photoelectron spectroscopy (XPS) by Senanayake et al. [9] shows a decrease in the oxygen and uranium binding energy, along with an increase in the rate of oxygen diffusion from the bulk to the surface, at temperatures greater than 400 K. Our group reported an increase in the DBAR line shape parameter between 400 and 500 K for a uranium sample with an oxide surface layer [8], indicating increasing vacancies due to oxygen desorption from the bulk to the surface which support Senanayake's findings.

In this paper, we discuss the methods used to measure the vacancy formation enthalpies and present new experimental and theoretical data supporting the notion that oxygen impurities lead to a lower measured value of the formation enthalpy. A comparison for measured and calculated vacancy formation enthalpies, as well as oxygen migration enthalpies, is also presented.

2. Methods and experiment

Uranium foil samples of 150 μm thickness were purchased from International Bio-Analytical Industries and cut into 4 cm^2 squares. The samples were mounted to a heating stage with Ta wire and placed in the mono-energetic positron beam line at Washington State University under a vacuum of 10^{-8} Torr. For the temperature scans, the beam energy was set to implant positrons at a mean positron implantation depth of 1.7 μm (66 keV). This value was calculated using [6],

$$<z> = \frac{40}{\rho}E^{1.6} \tag{1}$$

where ρ is the density in g/cm^3 and E is the energy of the positron beam in keV, <z> is given in nm. The samples were heated to various temperatures at heating rates of 1 K/min, and cooled to room temperature at the same rate. For a more detailed description of the samples and the beam line, please see Ref. [8].

Uranium has a high atomic number and the positron implantation energies used varied up to 70 keV. Because of this and the positron backscattering probability increases with atomic number and incident energy, there is a probability incoming positrons will scatter from the surface of the uranium sample and annihilate elsewhere producing a perturbed radiation peak that is not a true representation of the uranium sample. To ensure the data collected were not distorted from positron backscattering, a coincidence measurement was performed with two high purity germanium detectors.

3. Theory background

3.1. Diffusion in uranium

The diffusion of atoms and vacancies in the bulk of a substrate can be modeled using Fick's 1st Law,

$$J = D\nabla\varphi \tag{2}$$

or Fick's 2nd law, also known as the diffusion equation,

$$\partial_t\varphi = D\nabla^2\varphi \tag{3}$$

Here J is the flux of the atoms, φ is the concentration of the diffusing atoms, and D is the temperature dependent diffusion coefficient that contains the diffusion mechanism activation energy. This will be discussed in further detail later. The solution to these equations is usually assumed to be separable into two functions, one function is time dependent and the other is spatially dependent. The solutions can be very complicated and are determined by initial boundary conditions. Assuming homogeneous radial diffusion of the vacancies, the solution to Equation (3) for constant temperatures is an infinite series of Bessel functions [10–12]. The lowest root of the Bessel function will be the dominant term and the complex function can be approximated as

$$C_v(t) \cong C_0\left[1 - \exp\left(\frac{-t}{\tau_D}\right)\right]. \tag{4}$$

Here $C_v(t)$ is the vacancy concentration at a given time, C_0 is the initial vacancy concentration, $\tau_D = \alpha^2 D$ is the characteristic time constant required to achieve a vacancy equilibrium. α^2 depends on the geometry and is the lowest root to the Bessel function solution that solves Equation (3). This equation assumes the vacancies originate from a source such as free surfaces, grain boundaries, or free dislocations. The diffusion coefficient, D, is temperature dependant and therefore Equation (4) is a function of time and temperature for constant geometry configurations.

3.2. Impurity migration

When mobile, impurities diffuse from the bulk to the surface and will eventually desorb from the material into vacuum where they are pumped away. This process will eventually remove a majority of the impurities from uranium, and leave vacancies in the bulk. The impurities need to acquire enough energy to become mobile in the bulk uranium. One way an impurity can acquire this energy is from thermal excitation. To describe impurity migration in uranium for the initial heating of the sample, we can utilize Equation (4) with D being the thermally activated macroscopic defect diffusion coefficient [13,14],

$$D = D_0 \exp\left(\frac{-H_m}{k_b T}\right). \tag{5}$$

Here D_0 is the pre-exponential factor containing the migration entropy, the attempt frequency, and the square of the jump distance. H_m, is the migration enthalpy, k_b is Boltzmann's constant, and T is the absolute temperature. Because impurities such as oxygen diffuse in uranium by vacancy hopping [13], the macroscopic diffusion coefficient is the product of the vacancy concentration and the atomic diffusion coefficient D_A [14],

$$D = C_v D_A, \tag{6}$$

When the sample is cooled down, however, there are few interstitials to fill in the newly created vacancies. This would leave the sample with more vacancies than it had initially.

3.3. Thermal vacancy formation

The previous section describes how vacancies can be created for an impurity-saturated sample. For the case of a sample treated so that very few impurities remain, the primary mechanism to create new vacancies is to thermally activate them by heating the sample. The thermally activated vacancy concentration is given by,

Table 1
Uranium phases.

Phase	Temperature (K)	Structure	Volume (Å^3)
α	Up to 941	Orthorhombic	83.005 ± 0.003
β	941–1048	Tetragonal	654.716 ± 0.003
γ	1048–1407	Body centered cubic	43.763 ± 0.006

$$C_v = C_v^0 \exp\left(\frac{-H_v^f}{k_b T}\right), \tag{7}$$

C_v is the concentration of vacancy defects, C_v^0 is the pre-exponential factor containing the vacancy formation entropy, H_v^f is the vacancy formation enthalpy, k_b is Boltzmann's constant, and T is the absolute temperature. A detailed explanation of using positron techniques for measuring vacancy formation enthalpies can be found in Ref. [10]. When the temperature increases, more vacancies appear at a faster rate, and, when the temperature is cooled, those vacancies are filled in by interstitials. We now turn our attention to techniques used to probe vacancies.

3.4. Positron annihilation spectroscopy

When positrons are implanted into a material, they are attracted to open spaces such as vacancies and voids. When the positrons are trapped in the open spaces, the lifetime (time before it annihilates with an electron) is increased and the annihilation radiation peak centered at 511 keV becomes narrower. Defining the line shape parameter (S-parameter) and the wing parameter (W-parameter) as is customary [6,7,11], we see an increase in the S-parameter (and a decrease in the W-parameter) indicates a higher concentration of vacancies and/or larger vacancies.

From Equation (7), there is a relation between the concentration of vacancies and the annihilation parameter,

$$C_v = \frac{\lambda_b}{\mu}\left(\frac{F(T) - F_b(T)}{F_v(T) - F(T)}\right). \tag{8}$$

Here μ is the specific positron trapping coefficient, C_v is again the concentration of vacancy defects, λ_b is the bulk annihilation rate, F(T) is either the temperature dependent S-parameter or the W-parameter, F_b is the chosen annihilation parameter for the bulk, and F_v is the annihilation parameter when all positrons annihilate in vacancies. Depending on the mechanism for creating vacancies, we combine Equations (5), (6) and (8), or Equations (7) and (8) to solve for F(T) as a function of temperature,

$$F(T) = \frac{F_b(T) + F_v(T)\xi_i \exp\left(\frac{-H_i}{k_b T}\right)}{1 + \xi_i \exp\left(\frac{-H_i}{k_b T}\right)}. \tag{9}$$

Here we have defined $\xi_f = C_v \mu \lambda_b^{-1}$, and $\xi_m = D_0 \mu (D_A \lambda_b)^{-1}$ as the modified pre-exponential factor for the vacancy formation (ξ_f) or impurity migration (ξ_m) respectively. H_i represents either the vacancy formation enthalpy (H_v^f) or the migration enthalpy (H_m). Extracting F_b(T) and F_v(T) from the data, and assigning H_i and ξ_i as fitting variables, Equation (9) was fit to the temperature dependent PAS data to find both H_v^f and H_m using the S and W parameters.

Increasing the temperature will increase the diffusion coefficient and the impurities will migrate in the sample at a rate determined by the temperature. As time evolves, the impurities may leave the sample into the vacuum and a vacancy saturation level will eventually be obtained. We can combine Equation (4) with Equation (8) to solve for the annihilation parameter as a function of time for vacancies caused by impurity migration,

$$F(t) = \frac{F_b + F_v \psi\left[1 - \exp\left(\frac{-t}{\tau_D}\right)\right]}{1 + \psi\left[1 - \exp\left(\frac{-t}{\tau_D}\right)\right]}. \tag{10}$$

Here we define $\psi = C_0 \mu \lambda_b^{-1}$, and τ_D is again the characteristic time constant as in Equation (4). To check the validity of the experimental data, we must compare the results to theoretical calculations.

4. Computational methods and results

Theoretical calculations were carried out to determine the vacancy formation enthalpy of metallic uranium in the α-U phase. The projector augmented wave (PAW) method [15] was applied within the density functional theory [16,17] framework in the Vienna *ab initio* Simulation Package (VASP) [18–20]. Calculations were performed using the Perdew-Wang (PW91) [21] generalized gradient approximation (GGA) description of the exchange–correlation. The uranium PAW pseudopotential with the $6s^2 6p^6 5f^3 6d^1 7 s^2$ valence electronic configuration and a [Xe,5d,4f] core was used. For the calculations, we considered an energy cutoff of 500 eV and the convergence with respect to the self-consistent iterations was "accepted" for a total energy difference between cycles lower than 1×10^{-5}eV.

The crystal structure of the α-U phase is a face-center orthorhombic structure with a conventional unit cell containing four atoms (A20 Strukturbericht designation, Cmcm space group and oC4 Pearson symbol). For our calculations, a 72 atom supercell ($3 \times 3 \times 2$ unit cells) was used. A relaxation for the entire supercell, allowing the atoms themselves to relax, and, also allowing the volume and shape of the supercell to change, was performed. These calculations were made for various k-point meshes ($3 \times 3 \times 3$, $6 \times 6 \times 6$ and $9 \times 9 \times 9$). The first results were the calculated equilibrium lattice parameters (a,b,c and y) and the volume per atom. The results obtained for these parameters were: $a = 2.810$ Å, $b = 5.867$ Å, $c = 4.905$ Å, and $y = 0.098$ (unitless internal parameter). The volume per atom calculated was 19.95 Å^3. These results are in excellent agreement with those calculated by Taylor [22] and measured by Barrett et al. [23].

With the aim to get a value for the vacancy formation enthalpy H_v^f, a mono-vacancy was introduced into a supercell and a structural relaxation of the atomic positions was performed. The formation energy for a monovacancy is defined as [24].

$$E_{vac}\boxdot = E(U_{N-1}\boxdot) + \frac{N-1}{N}E(U_N), \tag{11}$$

where $E(U_{N-1}\boxdot)$ is the total energy of an (N-1) uranium supercell containing a monovacancy, and $E(U_N)$ is the total energy of an ideal uranium supercell containing N lattice sites. To guarantee a good convergence of the H_v^f value, different k-points meshes were tested. Specifically, $6 \times 6 \times 6$, $9 \times 9 \times 9$ and $11 \times 11 \times 11$ Monkhorst-Pack k-point meshes were used. The vacancy formation enthalpy was calculated to be 1.98eV. When the local density approximation (LDA) of Ceperley and Alder [25,26] was used for our calculations, the vacancy formation enthalpy was 2.22 eV. In general for pure metals, the LDA gives higher values for the vacancy formation enthalpy than the GGA does; in some cases (e.g. Pt, Pd and Mo), the difference is significant, up to 30–40% [27].

To understand the influence of the oxygen on the vacancy formation enthalpy, we calculated H_v^f in an oxygen doped α-uranium supercell. To this aim, we choose two different positions for the O atom impurity: i) a vacancy near an O substitutional, and ii) a vacancy near an O interstitial.

i) We create an oxygen doped α-uranium supercell by substituting one of the uranium atoms by an oxygen atom. Then a vacancy was created by removing one neighboring uranium atom.

ii) We introduce an impurity O atom in an interstitial position in the same crystal structure described above. Specifically, we added an O atom in the I4 interstitial position, (0.5, 0.2904, 0.3830) of the primitive α-uranium cell usually called "the free space defect" [28,29]. In a second step, following the procedure described in i), a vacancy was created in the supercell by removing one uranium atom neighboring the oxygen interstitial atom.

For the case i), (O substitutional) the vacancy formation enthalpy value obtained for the oxygen-doped vacancy using GGA was 1.7 eV. For case ii), (O interstitial) the calculated value of H_v^f strongly diminishes to 0.8 eV. Summarizing, the presence of one O impurity atom neighbor to a vacancy in the α-uranium supercell implies a noticeable diminution of the vacancy formation enthalpy from 1.98eV for pure uranium to 1.7eV and 0.8eV for substitutional and interstitial oxygen impurities.

5. Experimental results

5.1. Migration enthalpy

The as-received sample was black in color indicating a surface oxide layer. The sample was placed in the beam line under vacuum and heated while positron data was collected. Fig. 1 was taken from Ref. [8] and shows the first 3 heating and cooling cycles. The sample was heated to 450 K and cooled to room temperature (RT), then heated to 600 K and cooled to RT, and finally heated to 800 K and cooled to RT. The increase in the S-parameter is an indication vacancies are being created with increasing temperature. Equation (9), with the migration energy and pre-exponential factor, was used to fit the data for increasing temperatures only as is shown by the green (in web version) line in Fig. 1.

These data show increasing vacancy concentrations and is interpreted as impurities, such as oxygen atoms, diffusing from the bulk, to the surface, and out into the vacuum, leaving vacancies in their place. Substituting $S_b = (0.443 \pm 0.002) + [(1.8 \pm 0.6) \times 10^{-6}]T$ and $S_v = (0.474 \pm 0.001)$ into Equation (9) we calculate a migration enthalpy of $H_m = (0.6 \pm 0.1)$eV. The W-parameter was fit with Equation (9) with W_b and W_v values of $(0.069 \pm 0.001) + [(6.3 \pm 0.1) \times 10^{-7}]T$, and (0.064 ± 0.001) respectively, to find $H_m = (0.60 \pm 0.04)$eV.

For a different as-received sample, the temperature was increased to 535 K in 25 min and held there for approximately 2 h (see red data in Fig. 2). During this time, the S value rose to a final value 7.2% greater than the as received bulk value. The data were fit to Equation (10) giving $\psi = 0.058 \pm 0.006$ and $\tau_D = 33 \pm 6$ min. Another as-received sample was held at 547 K for 1.3 h (see Black data in Fig. 2). The data were fit again to Equation (10) giving $\psi = 0.063 \pm 0.001$ and $\tau_D = 26 \pm 5$ min. Since $\tau_D = \alpha^2 D$, we can combine this with Equation (8) to solve for the migration enthalpy a.different way [11],

$$\frac{\tau_1}{\tau_2} = \exp\left[\frac{-H_m}{k_b}\left(\frac{1}{T_1} - \frac{1}{T_2}\right)\right]. \quad (12)$$

When we use $T_1 = 535$ K and $T_2 = 547$ K along with their calculated time constants (τ_1 and τ_2), we find $H_m = (0.5 \pm 0.2)$ eV. This agrees well with the migration enthalpy calculated using Equation (10). Heat cycling the sample up to 800 K did not change the amount of vacancies in the material; however, these vacancies were removed once the sample was annealed at higher temperatures. This is discussed in the next section.

5.2. Vacancy annealing

Once the sample was heated to 800 K and cooled to RT, subsequent heat cycling of the sample from RT to 800 K did not change the amount of vacancies in the sample when measured at RT (see Fig. 1). Once the sample was heated to a temperature past its first phase transition (see Fig. 3-A and -B), we see the bulk S-parameter (W-parameter) is lower (higher), indicating the vacancies created by impurities are now being annealed out of the sample. After the sample was heated past its second phase transition temperature, the bulk S-parameter (W-parameter) is even lower (higher) still.

The S vs. W plot is a good way of determining the number of defect types in a material [29]. Each different slope in the SW plot represents a different defect type in the sample. In Fig. 4, we see the energy dependent SW plots of the data from Fig. 3A and B. These

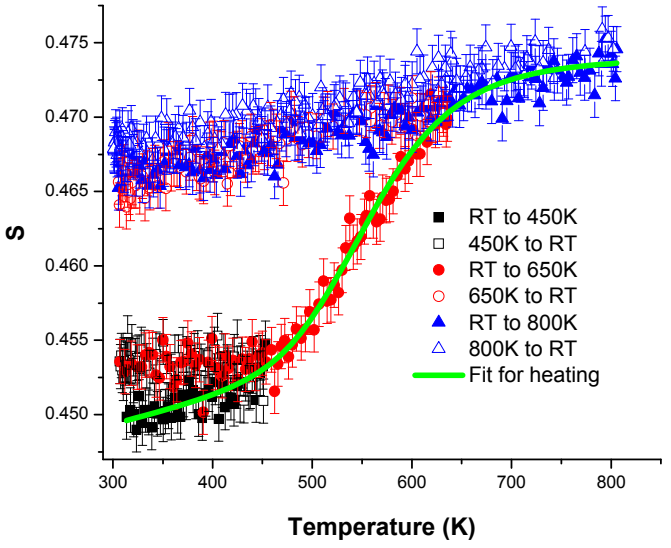

Fig. 1. S vs. T plot taken from Ref. [8] showing the first three heat cycles for an as-received sample. A clear hysteresis develops after heating where the number of vacancies increases. A migration enthalpy of 0.6 ± 0.1 eV was fit to the data for only increasing temperatures.

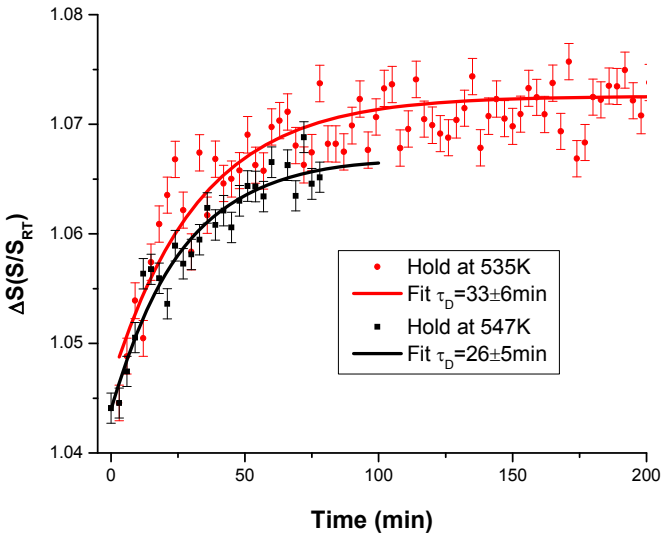

Fig. 2. S vs. time for as received samples heated to 535 K (red circles) and 547 K (black squares). The corresponding fit to Equation (10) is laid over top the data. (For interpretation of the references to colour in this figure legend, the reader is referred to the web version of this article.)

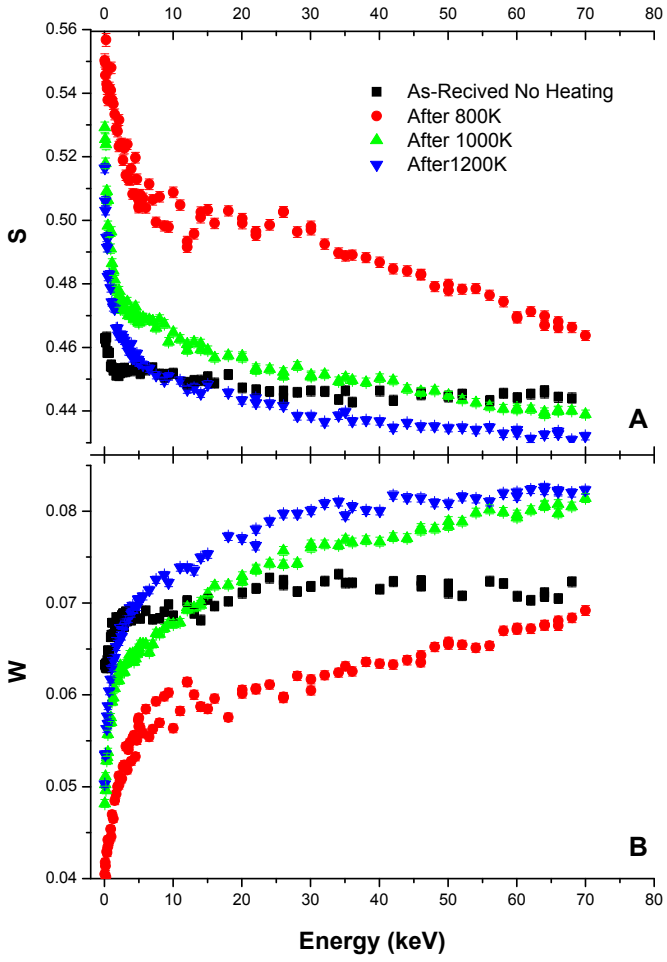

Fig. 3. A (Top). S vs. E plot taken from Ref. [8] showing different annealing temperatures remove more vacancies. **B (Bottom)**. Corresponding W vs. E for figure 3-B of the same data set displayed in Figure 3-A for the different annealing temperatures.

data are a function of positron implantation depth. The as-received sample data fall on a single slope line indicating the sample was homogeneous for the depths we were able to probe (up to 1.7 μm). When the sample was heated to 800 K and the bulk vacancies increased, we see the SW slope has changed, indicating the defect type changes after heating to 800 K.

For the samples annealed beyond the first and second phase transition temperatures, we see parallel slopes for both annealing treatments, different from the as-received and 800 K slope. The temperature dependent SW plot for a sample annealed to 1200 K was shown to have one slope for all three phases indicating a single defect type [8].

The bulk S value was measured at RT after being annealed at different temperatures up to 1270 K (see Fig. 5). This graph shows heating the sample to the first phase transition will create vacancies. Then, when the sample is heated to the β-phase, the vacancies begin to anneal out. Holding a sample at the β-phase lowered the S value to 0.4598 ± 0.0002 (only 0.4% higher than the as-received RT bulk value) in 2.5 h.

After heating to temperatures past the second phase transition into the γ-phase, the S-parameter is now lower than the as-received bulk S value.

5.3. Vacancy formation enthalpy

Sample A from Figs. 1 and 4 was heated again to 1200 K (see

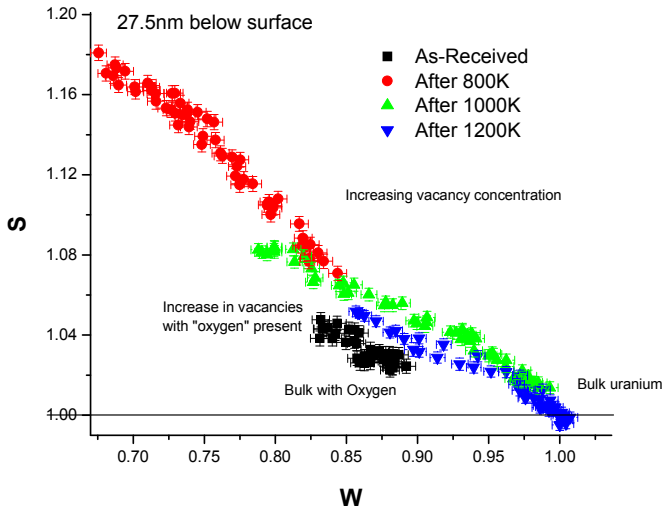

Fig. 4. Energy dependent S vs. W plot of different annealing temperatures.

black squares in Fig. 6). This time we do not see a rise in the S-parameter until a temperature of 800 K. This shows the vacancies created in Fig. 1 (red squares (in web version) in Fig. 6) are due to oxygen (and other impurities) leaving the uranium and not from thermally activated vacancies. Because the oxygen impurity migration enthalpy is lower than the thermally activated vacancy formation enthalpy, any impurities left in the sample will create vacancies at lower temperatures and shift the activation curve to lower temperatures resulting in a lower measured vacancy formation enthalpy.

To determine the effects of residual oxygen, a new sample was annealed in vacuum up to 1200 K and cooled to RT. The sample was heated two more times to 1200 K while taking PAS data (see Fig. 7-A and -B). We see both the S and W parameters vs. temperature at 1.7 μm below the samples surface are offset from each other. The second annealing cycle shows an increase (decrease) in S (W) at a lower temperature than the third cycle. The lines overlying the points in Fig. 7-A and -B are the fits from Equation (9).

The corresponding bulk and vacancy S-parameters for the second 1200 K annealed sample are $S_b = (0.4345 \pm 0.0005) + [(6.48 \pm 0.91) \times 10^{-6}]T$ and $S_v = (0.462 \pm 0.003)$ which results in a vacancy formation enthalpy of (0.57 ± 0.02) eV. The bulk and vacancy W-parameters for the first 1200 K annealed sample are $W_b = (0.0766 \pm 0.0005) - [(2.1 \pm 0.1) \times 10^{-7}]T$ and $W_v = (0.074 \pm 0.002)$ resulting in a vacancy formation enthalpy of (0.90 ± 0.02) eV.

The third annealed data bulk and vacancy S-parameters used in the formation calculation were $S_b(T) = [(1.4 \pm 0.1) \times 10^{-5}]T + (0.4325 \pm 0.0063)$, and $S_v = (0.461 \pm 0.002)$, leading to a measured vacancy formation enthalpy of (1.6 ± 0.2) eV. The bulk and vacancy W-parameters for the second 1200 K anneal were $W_b = -[(2.8 \pm 0.4) \times 10^{-6}]T + (0.0778 \pm 0.0002)$, and $W_v = (0.0668 \pm 0.0002)$, leading to a measured vacancy formation enthalpy of (1.46 ± 0.08) eV.

One sample was etched in nitric acid for 10 min to remove the oxide layer and then quickly placed in the vacuum chamber. As mentioned before, the as-received sample was black in color, but after etching it was silver and gray. This sample was heated the same way as the others described above. There were no increases in the S-parameter until the temperatures reached 750–800 K. From this data, a formation enthalpy of (1.6 ± 0.3) eV was calculated from the S-parameter data.

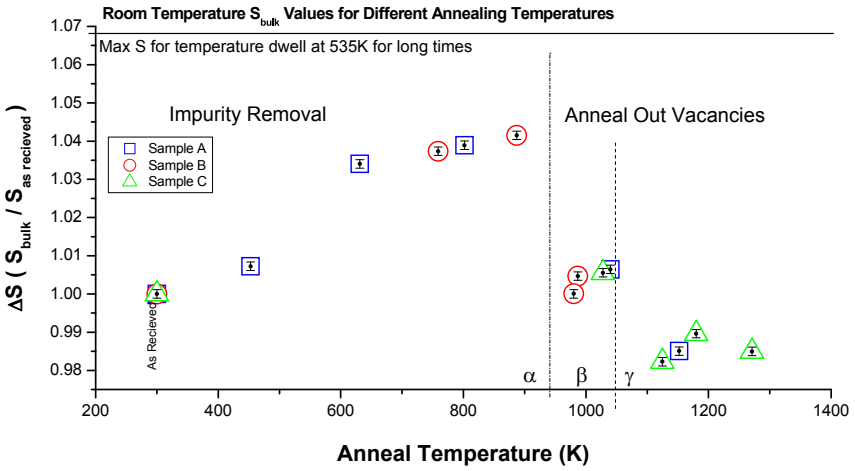

Fig. 5. Normalized room temperature bulk S values taken for three different samples after being isochronally heated at different temperatures. In all samples the heating rate was 1 K/min, the sample remained at the target temperature for 5 min, then was cooled at 1 K/min. Sample A is the sample shown in Fig. 1. At temperatures below the first phase transition we see the removal of impurities leaves vacancies as indicated by the increase in S. only after the sample was heated past the first phase transition, the S-parameter began to decrease, indicating annealing the vacancies away.

5.4. Coincidence Doppler broadening

The positron backscattering probability increases with atomic number and incident energy [29]. Because we are analyzing uranium at 66 keV and the sample is surrounded with titanium and tantalum heat shields, coincidence measurements were performed to ensure the annihilation parameters calculated are indeed from the uranium sample and not from backscattered positrons annihilating elsewhere or from photons scattering from the surrounding environment. The coincidence measurement was taken after annealing past 1200 K and the S bulk value was only 0.3% different from that taken without coincidence which is much smaller than the measurement error of 1.0%.

6. Discussion

Table 2 displays vacancy formation enthalpies of annealed uranium from three different PAS experiments. The volume of the uranium sample is also displayed for comparison. We see the smaller sample produced a larger measured value for the vacancy formation enthalpy. The value we report in Table 2 is the average obtained from measuring a total of five different samples. Four of the samples were heated in vacuum to remove the oxide layer, and 1 sample etched in nitric acid.

Many groups have used various theoretical methods to obtain values of uranium and uranium oxide properties [15–43]. Recent theoretical calculations are summarized in Table 3 and compared to our work.

This work shows if there are remaining impurities in the sample, they will migrate by vacancies from the bulk to the surface and will lower the measured formation enthalpy. There remains the possibility that the impurities could be trapped at grain boundaries, but this would not be seen by positrons unless the diffusion length is on the order of the size of the grain boundary.

Because of the size of the samples used by Matter et al. and Kögel et al., we believe they were not able to remove all of the impurities from their uranium samples. We do not claim to have removed 100% of the impurities in our sample, but because of our much smaller size, we believe that our percent of impurities is much lower. This would explain why their measured vacancy formation enthalpies were much lower than our reported value obtained by using a much smaller sample.

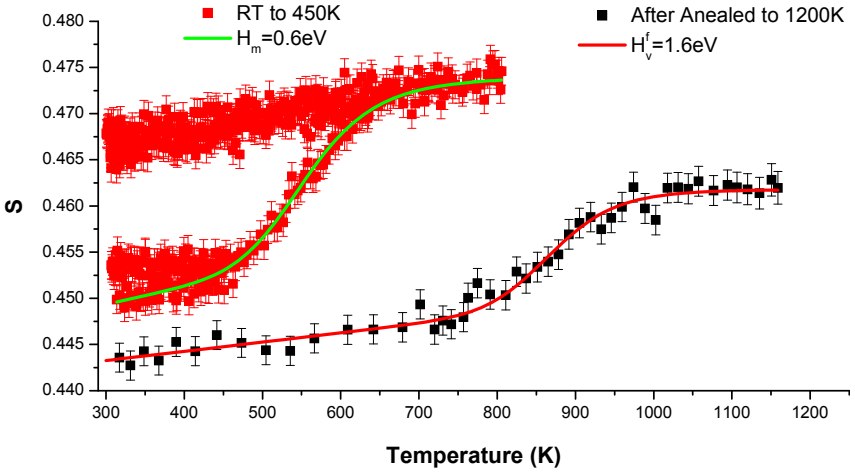

Fig. 6. S vs. T data for Sample A and data fit to Equation (9) of the same sample after being annealed at 1200 K giving an H_v^f of (1.6 ± 0.2)eV.

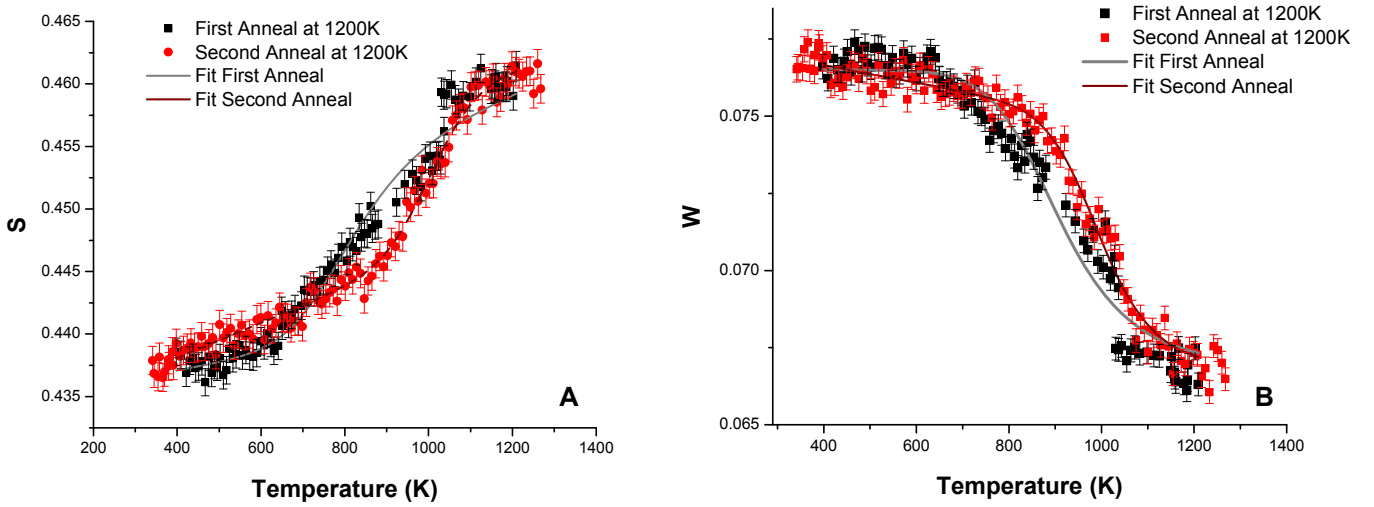

Fig. 7. A (Left). S vs. T plot with beam energy of 66 keV, 1.7 μm below the surface, and fit of Equation (9) using the S-parameter. There is a 64% difference in the measured H_v^f for a sample containing residual oxygen. **B (Right).** W vs. T plot with beam energy of 66 keV, 1.7 μm below the surface, and fit of Equation (9) using the W-parameter. This time there is a 50% difference in the measured H_v^f for a sample containing residual oxygen impurities.

Table 2
Experimental Formation Enthalpy using PAS.

Source	H_v^f (eV)	Sample volume (mm^3)
This work	1.6 ± 0.2	60
Matter	1.2 ± 0.25	3015
Kögel[a]	0.3	3451

[a] Error not reported.

Matter et al. and Kögel et al. also reported discontinuities in their data at phase transition temperatures. They both stated the discontinuities in the annihilation data were correlated to the discontinuities in the linear thermal expansion of uranium. Their data show a larger jump in the annihilation radiation between the β to γ phase transition than between the α to β.

However, in the data summary in Touloukian et al. [3] there is a larger jump in the linear expansion between the α to β phase transition than between the β to γ phase transition. From Fig. 7-A and -B, we only see larger discontinuities for the data with residual oxygen leading us to believe oxygen could play a role in the phase transformation of uranium.

We did not directly measure oxygen leaving the system but our work has shown at temperatures of 450 K impurity migration increases; this matches the results from Senanayake et al. where they show an increase in the rate of oxygen diffusion from the bulk to the surface. The same paper shows XPS data of polycrystalline U metal with a surface oxide layer consisting of mainly UO_2 that was successively annealed at 800 K for 30 min at a time. They concluded that oxygen was diffusing from the bulk to the surface, then into vacuum, resulting in a partial restoration of the U metal. It is possible that if they were to anneal at higher temperatures, like we did, they could have seen a full restoration of the U metal.

Table 3
Calculated formation enthalpy.

Source/Year	H_v^f (eV)	Method
This work	1.98[a]/2.22[b]	DFT–PAW
Beeler/2012	1.61	MEAM
Taylor/2008	1.95	DFT–PAW

DFT, density functional theory.
MEA, modified embedded-atom method interatomic potential.
PAW, with projector augmented wave pseudopotentials.
[a] GGA, generalized gradient approximation.
[b] LDA, local density approximation.

Our measured characteristic time constant for impurity vacancy creation was 33 min at a temperature of 535 K and 26 min at a temperature of 547 K. As expected from theory and seen in Fig. 2, the time constant will be longer at lower temperatures and shorter at higher temperatures. Since the heating rate for the sample in Figs. 1 and 6 was 1 K/min and the time constant between 450 K and 650 K varied by two orders of magnitude, we expect the higher temperature data in Fig. 6 will be distorted from the time evolution part of the solution to the diffusion equation.

This distortion would lead to a greater curvature at higher temperatures and cause the fitting algorithm to produce a larger pre-exponential and a lower migration energy and formation enthalpy. Thus, our reported values for the migration and formation enthalpies are a lower limit of the true value. This supports the VASP calculation that is 23% greater than the PAS measurement.

Fig. 7-A and -B show there is a 50–65% lower measured formation enthalpy during heating after the oxide layer has been removed but when oxygen and impurities are still desorbing from the bulk of the sample to the surface. This is supported by our recent calculations where the enthalpy is lowered by 23% when oxygen is introduced substitutionally into the lattice and 64% when oxygen is introduced into the lattice interstitially.

We were unable to find a direct comparison for oxygen migration in U metal in the literature but, our measured migration enthalpy is comparable with the previously measured value obtained by Kim et al. [28] where they used ^{18}O as a tracer to measure oxygen migration enthalpy in sub-stoichiometric UO_{2-X} to be $H_m = (0.51 \pm 0.1)$eV. It is interesting to point out that the migration enthalpies of UO_{2+X}, UO_2, and UO_{2-X} are reported by Murch et al. to be 0.64, 0.52, and 0.51 eV.

7. Conclusion

PAS measurements and VASP calculations were used to show oxygen impurities are responsible for lower measured values of vacancy formation enthalpies. We have calculated the H_v^f for polycrystalline depleted uranium using PAS techniques and compared our results to previously reported values. The average H_v^f

of a well annealed U metal when fitting the PAS S and W parameters was 1.6 ± 0.2 eV. This value is a lower limit to the actual value because of the time evolution contribution and is lower than the actual formation enthalpy. It is in reasonable agreement with previously reported theoretical values and our more recent VASP calculation of 1.98 eV. The oxygen migration enthalpy was measured to be 0.6 ± 0.1 eV which is also a lower limit of the true value.

The vacancies left after removing impurities by heating the samples between RT to the first phase transition temperature are reduced once the sample is heated past the first phase transition temperature as indicated by the decrease in the PAS S-parameter. Further heating to the second phase transition reduces the S-parameter further indicating fewer vacancies or changes to the positron interaction with the bulk uranium.

The two detector coincidence PAS measurements could be used in the future to identify the impurity-vacancy chemistry. Positron lifetime as a function of the uranium temperature could be used to identify the vacancy type. In order to measure a more accurate value of the formation enthalpy, a pure single crystal sample of metallic U needs to be measured. A pure single crystal sample of UO_2 could be used to accurately measure the oxygen migration enthalpy. Finally, it would be of interest to measure the H_v^f of uranium alloys used in reactor design such as U–Mo and U–Zr.

Acknowledgments

We acknowledge Idaho National Laboratory for funding under contract number 00014002, Agencia Nacional de Promoción Científica y Tecnológica (Argentina) (PICT 2011-1088), and Consejo Nacional de Investigaciones Científicas y Técnicas (Argentina) (PIP 112-201101-00793) as well as Narendra Parmar and Ryan Stewart for their discussions and help in the lab.

References

[1] H. Matter, J. Winter, W. Triftshäuser, J. Nucl. Mater. 88 (1980) 273–278.
[2] G. Kögel, P. Sperr, W. Triftshäuser, S. Rothman, J. Nucl. Mater. 131 (1985) 148–157.
[3] T.S. Touloukian, Thermophys. Prop. Matter 12 (1975) (Plenum, New York).
[4] P. Soderlind, Adv. Phs. 47 (1998) 959.
[5] B. Beeler, C. Deo, M. Baskes, M. Okuniewski, J. Phys. Condens. Matter 24 (2012), 075401 9.
[6] P.J. Schultz, K.G. Lynn, Rev. Mod. Phys. 60 (1988) 3.
[7] R.W. Siegel, Ann. Rev. Mater. Sci. 10 (1980) 393–425.
[8] K.R. Lund, K.G. Lynn, M.H. Weber, M.A. Okuniewski, J. Phys. Conf. Ser. 443 (2013) 012021.
[9] S.D. Senanayake, G.I.N. Waterhouse, A.S.Y. Chan, T.E. Madey, D.R. Mullins, H. Idriss, J. Phys. Chem. C 111 (2007) 7963–7970.
[10] H.E. Schaefer, Phys. Stat. Sol. A 102 (1987) 47.
[11] D.N. Seidman, R.W. Balluffi, Phys. Rev. 139 (1965), 6A 1824.
[12] F.S. Ham, J. Appl. Phys. 30 (6) (1958) 915.
[13] G.E. Murch, Diffus. Defect Data 32 (1983) 9–19.
[14] A.L. Laskar, Diffusion in Materials, Kluwer Academic Publishers, 1990, pp. 187–202.
[15] P. Blochl, O. Jepsen, O. Anderson, Phys. Rev. B 49 (1994) 16223.
[16] P. Hohenberg, W. Kohn, Phys. Rev. 136 (1964) B864.
[17] W. Kohn, L. Sham, Phys. Rev. 140 (1965) A1133.
[18] G. Kresse, J. Furthmuller, Phys. Rev. B 54 (1996) 11169.
[19] G. Kresse, D. Joubert, Phys. Rev. B 59 (1999) 1758.
[20] P. Blochl, Phys. Rev. B 50 (1994) 17953.
[21] J. Perdew, Y. Wang, Phys. Rev. B 45 (1992) 13244.
[22] C. Taylor, Phys. Rev. B 77 (2008) 094119.
[23] C. Barrett, M. Mueller, R. Hitterman, Phys. Rev. B 129 (1963) 625.
[24] C. Wolverton, Acta Mater. 55 (2007) 5867.
[25] D.M. Ceperley, B.J. Alder, Phys. Rev. Lett. 45 (1980) 566.
[26] J.P. Perdew, A. Zunger, Phys. Rev. B 23 (1981) 5048.
[27] T.R. Mattsson, A.E. Mattsson, Phys. Rev. B 66 (2002) 214110.
[28] Y. Li, T. Shan, T. Liang, S.B. Sinnott, S.R. Phillpot, J. Phys. Condens. Matter 24 (2012), 235403 (12 pp.).
[29] B. Beeler, B. Good, S. Rashkeev, C. Deo, M. Baskes, M. Okuniewski, J. Nucl. Mater. 425 (2012) 2.
[30] K. Kim, D. Olander, J. Nucl. Mater. 102 (1981) 192.
[31] S. Eichler, J. Gebauer, F. Börner, A. Polity, R. Krause-Rehberg, E. Wendler, et al., Phys. Rev. B 56 (3) (1997) 1393–1403.
[32] J. Makine, S. Palko, J. Martikainen, P. Hautojarvi, J. Phys. Condens. Matter 4 (1992) L503–L508.
[33] B. Dorado, P. Garcia, G. Carlot, C. Davoisne, M. Fraczkiewicz, B. Pasqet, et al., Phys. Rev. B 83 (2011) 035126.
[34] H. Fukushima, M. Doyama, J. Phys. F. Metal. Phys. 9 (1979) 10.
[35] J. Dryzek, J. Kuriplach, E. Dryzek, C.A. Quarles, M. Sob, Solid State Commun. 111 (9) (1999) 465–470.
[36] H. Labrim, M.F. Barthe, P. Desgardin, T. Sauvage, G. Blondiaux, C. Corbel, et al., Appl. Surf. Sci. 252 (2005) 3256–3561.
[37] S. Xiang, H. Huang, L. Hsiung, J. Nucl. Mater. (2008) 375113.
[38] B. Beeler, B. Good, S. Rashkeev, C. Deo, M. Baskes, M. Okuniewski, J. Phys. Condens. Matter 22 (2010), 505703 (7 pp.).
[39] T. Arima, K. Yoshida, K. Idemitsu, Y. Inagaki, I. Sato, IOP Conf. Ser. Mater. Sci. Eng. 9 (2010) 012003.
[40] F. Gupta, A. Pasturel, G. Brillant, Phys. Rev. B 81 (2010) 014110.
[41] A.S. Cooper, ACTA Cryst. 15 (6) (1962) 578–583.
[42] J. Thewlis, Nature 168 (4266) (1951) 198–199.
[43] G.E. Murch, C.R.A. Catlow, J. Chem. Soc. Faraday Trans. 2 83 (1987) 1157.